

## Phase Coherent Precessional Magnetization Reversal in Microscopic Spin Valve Elements

H. W. Schumacher,<sup>1,\*</sup> C. Chappert,<sup>1</sup> P. Crozat,<sup>1</sup> R. C. Sousa,<sup>2</sup> P. P. Freitas,<sup>2</sup> J. Miltat,<sup>3</sup> J. Fassbender,<sup>4</sup> and B. Hillebrands<sup>4</sup>

<sup>1</sup>*Institut d'Electronique Fondamentale, UMR 8622, CNRS, Université Paris Sud, Bâtiment 220, 91405 Orsay, France*

<sup>2</sup>*Instituto de Engenharia de Sistemas e Computadores, Rua Alves Redol, 9, P-1000 Lisboa, Portugal*

<sup>3</sup>*Laboratoire de Physique des Solides, CNRS, Université Paris Sud, Bâtiment 510, 91405 Orsay, France*

<sup>4</sup>*Fachbereich Physik, Universität Kaiserslautern, Erwin-Schrödinger-Straße 56, 67663 Kaiserslautern, Germany*

(Received 3 June 2002; published 3 January 2003)

We evidence multiple coherent precessional magnetization reversal in microscopic spin valves. Stable, reversible, and highly efficient magnetization switching is triggered by transverse field pulses as short as 140 ps with energies down to 15 pJ. At high fields a phase coherent reversal is found revealing periodic transitions from switching to nonswitching under variation of pulse parameters. At the low field limit the existence of a relaxation dominated regime is established allowing switching by pulse amplitudes *below* the quasistatic switching threshold.

DOI: 10.1103/PhysRevLett.90.017201

PACS numbers: 75.60.Jk, 85.70.Kh

It has been well known since the 1950s that the ultrafast dynamics of the magnetization are governed by damped precession of the magnetization about a local effective field  $H_{\text{eff}}$ . The corresponding equation of motion is the so-called Landau-Lifshitz-Gilbert equation  $d\mathbf{M}/dt = -\gamma(\mathbf{M} \times \mathbf{H}_{\text{eff}}) + (\alpha/M_s)(\mathbf{M} \times d\mathbf{M}/dt)$ , with  $\mathbf{M}$  being the magnetization vector,  $\gamma$  the gyromagnetic ratio,  $\alpha$  the Gilbert damping parameter, and  $M_s$  the saturation magnetization [1]. A fast rising field pulse  $\mathbf{H}_{\text{pulse}}$  applied perpendicular to  $\mathbf{M}$  generates a large torque  $-\gamma(\mathbf{M} \times \mathbf{H}_{\text{pulse}})$ , thus inducing a pronounced precession of  $\mathbf{M}$  [2–5]. Using this precession to *switch* the magnetization [6–11] promises a high energy efficiency together with ultrafast reversal times reaching the fundamental limit of a half precession period [8,9]. In first experiments intense magnetic field pulses of only a few ps duration were used to reverse large domains in Co and Co/Pt thin films [6,7]. Numerical studies [8,9] also predicted precessional switching in small magnetic cells as used in magnetic random access memories (MRAM) [12]. Transverse pulses of technically available durations around 100 ps should induce magnetization switching characterized by periodic transitions from switching to nonswitching under variation of pulse parameters. Recently, observations of precessional switching in magnetic cells by hard axis pulses in the limit of high pulse amplitudes and short pulse duration have been reported [13,14]. However, the periodic behavior fully proving the precessional nature of the reversal has not been observed.

Here we experimentally evidence the coherent periodic precessional switching in microscopic memory cells by ultrashort transverse field pulses. The observed switching periodicity is fully linked to the characteristic time scales of the underlying precession. Furthermore, for low fields we find a novel Gilbert damping dominated reversal regime allowing highly efficient switching by fields below the hard axis anisotropy field, i.e., *below* the quasistatic switching threshold.

The experiments are carried out on exchange biased spin valves (SV) consisting of Ta 65 Å/Ni<sub>81</sub>Fe<sub>19</sub> 40 Å/Mn<sub>78</sub>Ir<sub>22</sub> 80 Å/Co<sub>88</sub>Fe<sub>12</sub> 43 Å/Cu 24 Å/Co<sub>88</sub>Fe<sub>12</sub> 20 Å/Ni<sub>81</sub>Fe<sub>19</sub> 30 Å/Ta 8 Å. The films are structured into  $2 \times 4 \mu\text{m}^2$  SV cells as shown in the inset of Fig. 1(a). The electrical contacts (C) overlap with the ends of the SV cell. Via the contacts the cell's current-in-plane giant magnetoresistance (GMR) is measured. The pinned magnetic layer is aligned along the easy magnetization axis (long SV dimension) by the exchange bias. Figure 1(a) shows an easy axis field ( $H_{\text{easy}}$ ) GMR loop. The loop exhibits a kink on the right and asymmetric characteristics of exchange bias [15]. Because of overlap of contacts and SV the GMR signal mainly probes the magnetization within the center of the cell. Flux closure domains underneath the contacts thus do not contribute to the loop. The loop is shifted to an offset field  $H_{\text{offset}} \approx 14$  Oe due to coupling of the pinned and the free layer [16]. Reversal of the free layer leads to a room temperature GMR change of 5.6% at  $H_{\text{easy}} = H_{\text{offset}}$ . Magnetic field pulses  $\mathbf{H}_{\text{pulse}}$  along the in-plane hard axis are generated by current injection through an integrated high-bandwidth pulse line [17]. The transient pulses are monitored using a 50 GHz sampling oscilloscope. The pulse durations  $T_{\text{pulse}}$  can be adjusted between 140 ps and 10 ns (at half maximum) with rise times down to 45 ps (from 10%–90%) and maximum fields around 240 Oe. In-plane static fields are applied via an external coil.

Field pulses are applied along the in-plane magnetic hard axis, i.e., perpendicular to the initial and final direction of  $\mathbf{M}$ , and the switching is expected to be symmetric; i.e., consecutive application of the *same* pulse should reversibly toggle  $\mathbf{M}$ . This is shown in Fig. 1(b). First, the sample is saturated into the low resistance (parallel) state by applying  $H_{\text{easy}} = -100$  Oe before increasing  $H_{\text{easy}}$  to  $H_{\text{offset}}$  to compensate the loop shift. The pulse response of the cell is then tested by consecutively applying identical hard axis pulses. In Fig. 1(b) the GMR

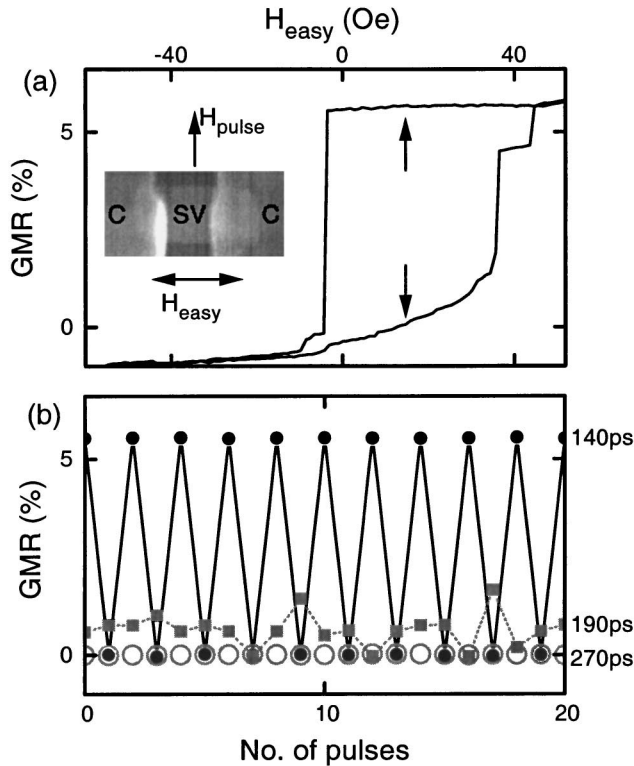


FIG. 1. Precessional switching of a  $2 \mu\text{m} \times 4 \mu\text{m}$  spin valve. Inset of (a): electron micrograph of a typical SV cell with electrical contacts (C). Static fields are applied along the easy (long) axis  $H_{\text{easy}}$  (horizontally), pulse fields  $H_{\text{pulse}}$  along the hard axis. (a) Easy axis GMR loop, GMR vs field. The relative GMR variation at  $H_{\text{offset}}$  is  $\Delta\text{GMR} = 5.6\%$ . (b) Precessional switching: GMR after each pulse vs pulse index.  $H_{\text{offset}}$  is compensated. Pulse parameters are  $T_{\text{pulse}} = 140$  ps,  $H_{\text{pulse}} = 155$  Oe (black, full circles); 190 ps, 195 Oe (gray squares); and 270 ps, 215 Oe (gray, open circles). The 140 ps toggles the magnetization with every pulse.

measured after each pulse is plotted vs the pulse index for three different pulse parameters. For  $T_{\text{pulse}} = 140$  ps,  $H_{\text{pulse}} = 155$  Oe (solid circles), each pulse toggles the magnetization. Each GMR change  $\Delta\text{GMR}$  of  $\pm 5.6\%$  corresponds to full reversal at  $H_{\text{offset}}$  [see arrows in 1(a)]. For slightly longer pulses ( $T_{\text{pulse}} = 190$  ps, 195 Oe: gray squares) reversible switching no longer occurs. Here the GMR changes stochastically between 0.01% and 1.5%. Finally, for 270 ps, 215 Oe pulses (open circles), the sample is always found in the parallel low resistance state (no switch), although  $H_{\text{pulse}}$  even slightly increased [18].

As mentioned earlier, the torque on  $\mathbf{M}$  is maximum when  $\mathbf{M}$  and  $\mathbf{H}_{\text{eff}}$  are oriented perpendicularly. In Fig. 2(a) such is the case right after the onset of the hard axis field  $\mathbf{H}_{\text{pulse}}$  and the torque  $-\gamma(\mathbf{M} \times \mathbf{H}_{\text{pulse}})$  induces a rotation of  $\mathbf{M}$  out of the film plane. This out-of-plane component, in turn, generates a strong demagnetizing field  $\mathbf{H}_D$  [19] also oriented perpendicular to the plane but pointing in the direction opposite to the  $z$  magnetization component [Fig. 2(b)]. Under the action

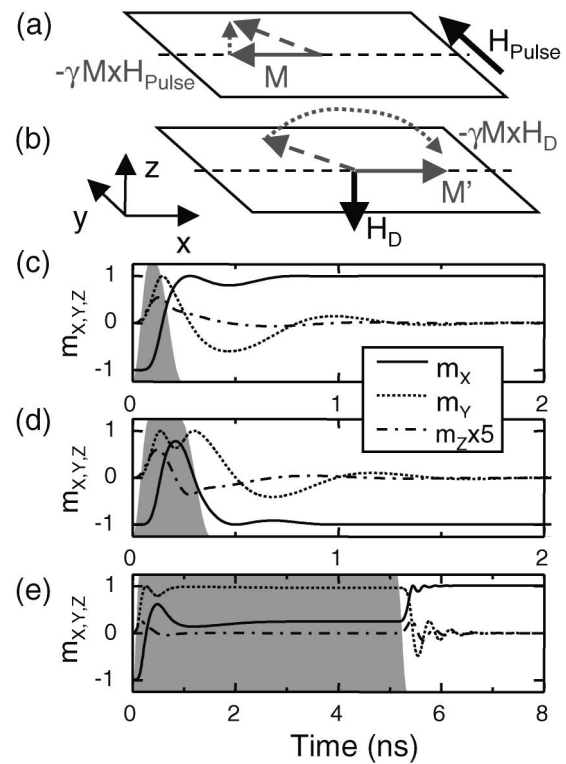


FIG. 2. (a),(b) Sketch of precessional switching: (a)  $\mathbf{M}$  is tilted out of plane by  $\mathbf{H}_{\text{pulse}}$ , and (b) rotates about the demagnetizing field  $\mathbf{H}_D$  towards  $\mathbf{M}'$ . (c)–(e) Macrospin simulations: Normalized components of  $\mathbf{M} = (m_x, m_y, m_z)$  vs time.  $m_z$  is increased by 5 for clarity. The gray background marks the pulse shape. (c) Reversal by a 140 ps pulse (cf. Fig. 1). (d) Nonreversal by a 270 ps pulse. (e) Relaxational reversal for a 5 ns, 55 Oe pulse.

of  $\mathbf{H}_D$ ,  $\mathbf{M}$  remains mainly in-plane, and  $\mathbf{H}_D$  and  $\mathbf{M}$  are still oriented almost perpendicular to each other allowing for fast quasi-in-plane rotation of  $\mathbf{M}$  under the action of the new torque  $-\gamma(\mathbf{M} \times \mathbf{H}_D)$ . If the pulse terminates at about a half of a precession period  $T_{\text{pulse}} \approx \frac{1}{2}T_{\text{prec}}$ , switching is expected. Also the reversibility of the switching by multiple unipolar pulses is well accounted for by these considerations. Indeed, a reversal of  $\mathbf{M}$  changes only the sign of the dipolar field  $\mathbf{H}_D$  leaving the reversal mechanism unchanged.

This can be substantiated by numerical simulations performed in the single spin approximation [8]. The free layer is modeled using  $4\pi M_s = 10\,800$  Oe of permalloy, demagnetization factors  $N_x = 0$  (easy axis),  $N_y/4\pi = 0.0067$  (in-plane hard axis),  $N_z/4\pi = 0.9933$  (out of plane) chosen to match the measured in-plane anisotropy field of  $H_A \approx 70$  Oe, and  $\alpha = 0.03$  as determined previously [17]. Last, the pulse shapes and fields mimic the measured transient pulses.

Figure 2(c) displays the calculated normalized components of  $\mathbf{M}$  vs time for the 140 ps pulse. The reversal is reproduced and the easy axis component  $m_x$  changes sign.

The nonzero  $m_z$  (out-of-plane) and thus the influence of  $\mathbf{H}_D$  are also seen. Precession is exemplified by the  $\pi/2$  phase shift between  $m_x$  and  $m_z$ . Furthermore,  $\mathbf{M}$  passes through an almost perfect alignment with the hard axis ( $m_x$  and  $m_z \approx 0$ ,  $m_y \approx 1$ ) confirming the quasi-in-plane rotation. Upon pulse termination  $\mathbf{M}$  finally relaxes towards the nearest attractor, namely  $m_x = 1$ .

The simulated nonreversal by the 270 ps pulse is shown in Fig. 2(d). As a consequence of the longer pulse duration  $m_x$  now oscillates to the reversed orientation *and* back before the pulse terminates and relaxation towards  $m_x = -1$  occurs. Therefore, in spite of the strong precessional motion of  $\mathbf{M}$ , no effective cell reversal takes place. Simulating the observed partial switching ( $T_{\text{pulse}} = 190$  ps) goes beyond the limits of our model; however, the weak reproducibility can be explained owing to the same picture. If the pulse decays when  $\mathbf{M}$  is oriented near the hard axis, i.e., near the energetic saddle point, a small trajectory variation may change the final attractor and thus induce a nearly stochastic reversal.

A further increase of  $T_{\text{pulse}}$  will lead to multiple oscillations of  $\mathbf{M}$  about  $\mathbf{H}_{\text{pulse}}$ . For strong pulses ( $H_{\text{pulse}} \gg H_A$ ) and weak damping, switching is expected whenever the pulse terminates out of phase with the precession, i.e., when  $T_{\text{pulse}} \approx (n + \frac{1}{2})T_{\text{prec}}$ ,  $n$  being an integer defining the order of the switching process. Contrarily, pulses with  $T_{\text{pulse}} \approx nT_{\text{prec}}$  will result in nonreversal of  $\mathbf{M}$ . Such phase coherent, higher order reversal is shown in Fig. 3 for a second, similar device. In Fig. 3(a) the degree of revers-

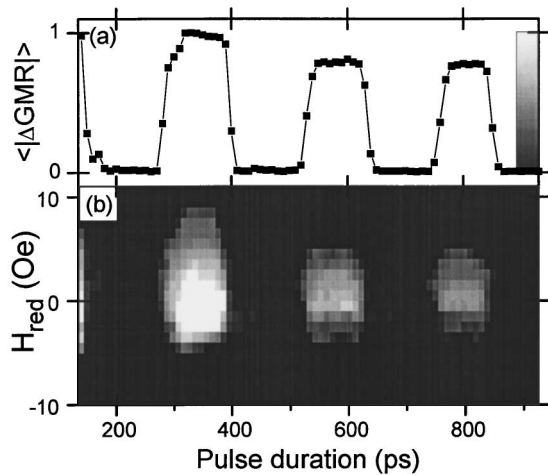


FIG. 3. Switching of a further  $2 \mu\text{m} \times 4 \mu\text{m}$  spin valve as a function of  $T_{\text{pulse}}$  and reduced easy axis field  $H_{\text{red}} = H_{\text{easy}} - H_{\text{offset}}$ .  $H_{\text{offset}} = 12$  Oe [18]. (a)  $\langle |\Delta\text{GMR}| \rangle$  the normalized average of  $|\Delta\text{GMR}|$  per pulse vs  $T_{\text{pulse}}$  at  $H_{\text{red}} = 0$ . Four regions of reversible switching are found ( $\langle |\Delta\text{GMR}| \rangle \approx 1$ ). (b) Gray-scale map of  $\langle |\Delta\text{GMR}| \rangle$  as a function of  $T_{\text{pulse}}$  and  $H_{\text{red}}$ . Legend is given in (a). Black:  $\langle |\Delta\text{GMR}| \rangle \leq 0.1$ , no reversible switching; white:  $\langle |\Delta\text{GMR}| \rangle \geq 0.9$  stable, large amplitude reversible switching, gray: intermediate values, instable or low amplitude switching. (a) is a section of (b) along  $H_{\text{red}} = 0$ .

ible switching,  $\langle |\Delta\text{GMR}| \rangle$ , is plotted vs  $T_{\text{pulse}}$ , and is shown in Fig. 3(b) in a gray-scale map as a function of  $T_{\text{pulse}}$  and the reduced easy axis field  $H_{\text{red}} = H_{\text{easy}} - H_{\text{offset}}$ .  $H_{\text{pulse}} = 230$  Oe [18].  $\langle |\Delta\text{GMR}| \rangle$  is the absolute resistance change per applied pulse normalized to full reversal, and averaged over a series of pulses.  $\langle |\Delta\text{GMR}| \rangle \approx 1$  indicates stable reversible switching, and 0 no switching.

Figure 3(a) shows  $\langle |\Delta\text{GMR}| \rangle$  for  $H_{\text{red}} = 0$ . Four regions of stable switching, well separated by stable nonswitching regions, are observed. Note again, the zero order switching ( $n = 0$ ) for the shortest accessible pulses of  $T_{\text{pulse}} = 140$  ps. In the adjacent region up to  $T_{\text{pulse}} \approx 280$  ps no switching takes place as  $T_{\text{pulse}} \approx T_{\text{prec}}$ . Higher order switching ( $n = 1, 2, 3$ ) is observed for  $T_{\text{pulse}} = 350, 590, 800$  ps. For  $n = 1$  full, stable switching is obtained. For higher reversal orders ( $n = 2, 3$ ),  $\langle |\Delta\text{GMR}| \rangle$  decreases due to less reliable and partial switching. Note that stable switching is observed over a relatively broad range of  $T_{\text{pulse}}$  of about 100 ps indicating a large tolerable phase mismatch of the coherent switching still allowing stable attraction to the reversed direction [20]. Also up to  $H_{\text{red}} \approx \pm 4$  Oe [Fig. 3(b)], corresponding to about 28% of the static coercivity ( $H_C = 14$  Oe),  $\mathbf{M}$  still reversibly switches ( $n = 0, 1$ ). However,  $|H_{\text{red}}| \geq 0.5H_C$  results in irreversible switching,  $\mathbf{M}$  ending up always aligned with  $H_{\text{red}}$  whichever its initial orientation.

These results are of vital importance for MRAM applications. The relatively broad pulse parameter range for coherent switching should, e.g., allow down scaling of the cells. Switching of each cell of an array by a given pulse seems possible despite an inevitable spread in cell parameters (e.g., due to shape variations). Moreover, bit addressing can be realized in the standard cross line architecture [12] using the irreversible switching at higher easy axis fields.

A characterization of the switching properties over a wide range of  $H_{\text{pulse}}$  and  $T_{\text{pulse}}$  is displayed in Fig. 4 for  $H_{\text{red}} = 0$ .  $\langle |\Delta\text{GMR}| \rangle$  (top) and the results of the simulations (bottom) are shown. The simulated field dependence of the coherent regimes is in good agreement with the measurements, and the minimum switching field of about 50 Oe is well reproduced. A decrease of  $H_{\text{pulse}}$  first shifts the switching regions towards larger values of  $T_{\text{pulse}}$ . This is expected from simple ferromagnetic resonance arguments since the precession period generally increases with decreasing field [19].

Just above the switching field limit of about 50 Oe, simulations predict  $n = 0$  switching *independent* of  $T_{\text{pulse}}$ . The coherence criterion appears to be no longer valid, however, now the condition  $H_{\text{pulse}} \gg H_A$  is no longer fulfilled.  $\mathbf{M}$  overcomes the hard axis only once during pulse application and precesses about an equilibrium direction defined by the ratio of  $H_{\text{pulse}}$  and  $H_A$  as seen in Fig. 2(e) for a 5 ns, 55 Oe pulse. The damping inhibits the oscillation back across the in-plane hard axis

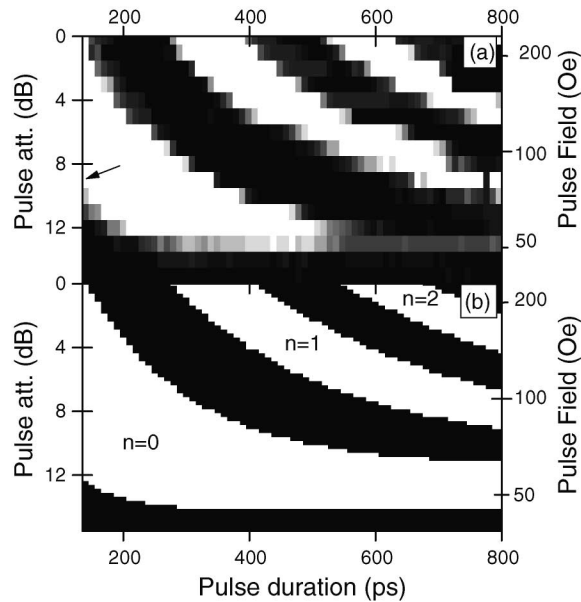


FIG. 4. Pulse field dependence of the precessional switching of the device of Fig. 3. (a)  $\langle |\Delta\text{GMR}| \rangle$  as a function of  $T_{\text{pulse}}$  and  $H_{\text{pulse}}$ .  $H_{\text{red}} = 0$  Oe. Black:  $\langle |\Delta\text{GMR}| \rangle \leq 0.1$ . White:  $\langle |\Delta\text{GMR}| \rangle \geq 0.8$ .  $H_{\text{pulse}}$  is attenuated in steps of 1 dB. Switch pulse energies are as low as 15 pJ (arrow). (b) Calculated switching map for the same device derived from macrospin simulations. Black: no switching; white: switching. The order  $n$  of switching is indicated.

and  $m_x$  changes sign only once. Thus, independently of  $T_{\text{pulse}}$ , switching will be completed through relaxation once the field decays. Note again that  $H_{\text{pulse}} < H_A$ ; i.e., contrary to previous statements [7,13] the switching fields can be lower than the classical quasistatic switching threshold. Experiments also provide evidence for such damping dominated relaxational switching with  $H_{\text{pulse}} \approx 50$  Oe  $< H_A$  for  $T_{\text{pulse}} = 300, \dots, 800$  ps. However,  $\langle |\Delta\text{GMR}| \rangle$  remains below 1 indicating only partial and instable switching. A reason for this is that for the given low  $\alpha$  this switching mode is limited to a narrow field range. Weak parameter inhomogeneity, due, e.g., to magnetic microstructure, might be sufficient to inhibit full reversal. Smaller cells with a more single-domain-like behavior and a larger  $\alpha$  might help stabilize this switching mode. Note that conversely, the coherent reversal regimes only weakly depend on  $\alpha$ , at least for  $n = 0$ . Last, with further reduction of  $H_{\text{pulse}}$  the precession amplitude becomes too weak to reach the in-plane hard axis and reversal is inhibited. Figure 4 also allows one to find parameters for optimal switching efficiency. Switching is obtained by pulses of  $T_{\text{pulse}} = 140$  ps and only 15 pJ energy (arrow) proving highly efficient when compared to conventional switching schemes [21,22].

To conclude, we have studied the precessional switching of magnetic memory cells as conceptually used in MRAMs. Ultrafast, reversible switching by hard axis pulses as short as 140 ps and with pulse energies down to 15 pJ was achieved. The existence of a phase coherent reversal regime at high fields, and a damping dominated, relaxational regime at low fields was established. In the latter, switching by pulse fields below the in-plane hard axis anisotropy field, i.e., below the quasistatic switching threshold was demonstrated.

We thank M. Bauer for fruitful discussions and acknowledge financial support by the European Union (EU) Marie Curie fellowship HPMFCT-2000-00540 and in part by the EU TMR under Contract No. ERBFMRX-CT97-0147 and by NEDO Contract "Nanopatterned Magnets."

\*Corresponding author.

Email address: schumach@ief.u-psud.fr

- [1] L. Landau and E. Lifshitz, *Phys. Z. Sowjetunion* **8**, 153 (1953); T.L. Gilbert, *Phys. Rev.* **100**, 1243 (1955).
- [2] W. K. Hiebert, A. Stankiewicz, and M. R. Freeman, *Phys. Rev. Lett.* **79**, 1134 (1997).
- [3] Y. Acreman *et al.*, *Science* **290**, 492 (2000).
- [4] T. M. Crawford *et al.*, *Appl. Phys. Lett.* **74**, 3386 (1999).
- [5] S. E. Russek, S. Kaka, and M. J. Donahue, *J. Appl. Phys.* **87**, 7070 (2000).
- [6] C. H. Back *et al.*, *Phys. Rev. Lett.* **81**, 3251 (1998).
- [7] C. H. Back *et al.*, *Science* **285**, 864 (1999).
- [8] M. Bauer *et al.*, *Phys. Rev. B* **61**, 3410 (2000).
- [9] J. Miltat, G. Alburquerque, and A. Thiaville, in *Spin Dynamics in Confined Magnetic Structures*, edited by B. Hillebrands and K. Ounadjela (Springer, Berlin, 2001).
- [10] J. Miltat and A. Thiaville, *Science* **290**, 466 (2000).
- [11] Y. Acreman *et al.*, *Appl. Phys. Lett.* **79**, 2228 (2001).
- [12] See, e.g., S. Tehrani *et al.*, *IEEE Trans. Magn.* **36**, 2752 (2000).
- [13] S. Kaka and S. E. Russek, *Appl. Phys. Lett.* **80**, 2958 (2002).
- [14] Th. Gerrits *et al.*, *Nature (London)* **418**, 509 (2002).
- [15] T. Ambrose and C. L. Chien, *J. Appl. Phys.* **83**, 7222 (1998).
- [16] D. Wang *et al.*, *IEEE Trans. Magn.* **36**, 2802 (2000).
- [17] H. W. Schumacher *et al.*, *Appl. Phys. Lett.* **80**, 3781 (2002).
- [18]  $H_{\text{pulse}}$  is constant for  $T_{\text{pulse}} > 300$  ps. Below, it decreases with  $T_{\text{pulse}}$  down to 65% due to limitations of the pulse generator.
- [19] C. Kittel, *Introduction to Solid State Physics* (Wiley, New York, 1976), 5th ed.
- [20] A large phase mismatch will result in pronounced precession of  $\mathbf{M}$  upon pulse termination. However, in the center of the switching regimes only weak ringing is expected.
- [21] R. H. Koch *et al.*, *Phys. Rev. Lett.* **81**, 4512 (1998).
- [22] B. C. Choi *et al.*, *Phys. Rev. Lett.* **86**, 728 (2001).